Pulmonary Stenosis

7

Contents

7.1 Anatomy and Haemodynamics

Obstruction of the right ventricular outflow tract and pulmonary artery may occur at the valvular, subvalvular or supravalvular level (Fig. 7.1). Pulmonary valvular stenosis is by far the most frequent modality of obstruction (Freedom and Benson 2004). In the majority of cases, valvular stenosis is caused by fusion of the commissures with consecutive reduction of the valvular orifice. Although stenotic bicuspid pulmonary valves have been described, in most instances, the valve will be tricuspid (Freedom and Benson 2004; Gerlis 1999). It has been well documented by fetal echocardiography that pulmonary valvular stenosis may develop during intrauterine life and can show progression until the time of delivery (Lemler and Ramaciotti 2009). A second, less frequent pathomechanism for pulmonary valvular stenosis is dysplasia and thickening of the valve leaflets (Freedom and Benson 2004). Since the latter valves do not exhibit fusion of the commissures, they are less suitable for effective treatment by surgical commissurotomy or by balloon angioplasty (Musewe et al. 1987). This type of valvular stenosis is commonly associated with additional supravalvular narrowing at the sinotubular junction. Pulmonary valvular stenosis due to dysplasia of the valve is frequently found in children with Noonan's syndrome (Burch et al. 1993; Duncan et al. 1981; Roberts et al. 2013; Romano et al. 2010). The incidence of pulmonary stenosis has been described as 6,1 % of congenital cardiac malformations (Lindinger et al. 2010; Schwedler et al. 2011).

Pulmonary valve stenosis is frequently associated with an interatrial communication presenting either as patent foramen ovale or secundum atrial septal defect. However pulmonary valvular stenosis may also be part of more complex lesions like tetralogy of Fallot or double outlet right ventricle.

Depending on the severity of the valvular obstruction, right ventricular systolic pressure increases, resulting in concentric hypertrophy of the right ventricle. In children with critical pulmonary stenosis, reduced antegrade flow through the right ventricular cavity during intrauterine life may result in moderate or even severe hypoplasia of the right ventricle

Electronic supplementary material The online version of this chapter (doi:10.1007/978-3-319-42919-9_7) contains supplementary material, which is available to authorized users.

M. Hofbeck et al., *Doppler Echocardiography in Infancy and Childhood*, DOI 10.1007/978-3-319-42919-9_7

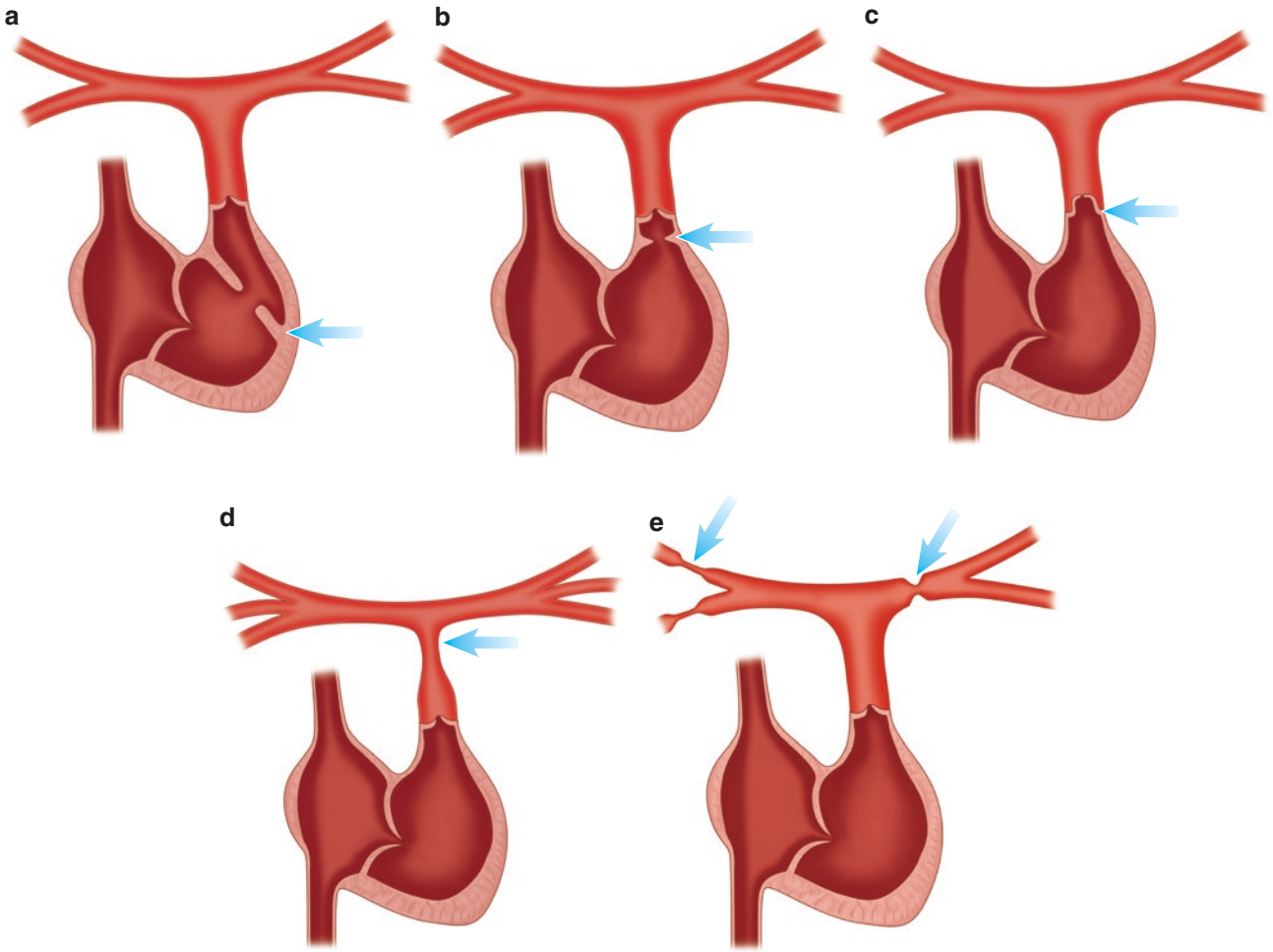

Fig. 7.1 Obstructions of the right ventricular outflow include subvalvular (**a**, **b**), valvular (**c**) and supravalvular (**d**, **e**) stenoses. Subvalvular obstruction may be located at subinfundibular (**a**) or infundibular level (**b**). Supravalvular obstructions may affect the main pulmonary artery (**d**) and the central or peripheral pulmonary arteries (**e**)

(Freedom and Benson 2004). Right ventricular morphology in these patients may resemble patients with pulmonary atresia and intact ventricular septum with attenuation of the apical portion and mild to moderate hypoplasia of the tricuspid valve (Freedom and Benson 2004). Significant long-standing pulmonary valve stenosis may produce secondary narrowing of the subpulmonary infundibulum which has to be distinguished from fixed infundibular stenosis: while secondary infundibular narrowing will regress following effective relief of the valvular obstruction, the latter will remain unaltered and has to be addressed surgically (Buheitel et al. 1999). Isolated infundibular stenosis is rare. It may be due to fibromuscular obstruction or hypertrophic cardiomyopathy (Lemler and Ramaciotti 2009). Infundibular obstruction, caused by anterior deviation of the infundibular septum, represents an integral part of tetralogy of Fallot (Chap. 11). Furthermore subvalvular obstruction by deviation of the infundibular septum may be encountered in other conotruncal anomalies like DORV (Chap. 14) (Martinez and Anderson 2005).

A different mechanism of subvalvular stenosis is present in patients with double-chambered (two-chambered) right ventricle (DCRV). In these patients, anomalous muscle bundles divide the right ventricle into a high pressure inflow and a low pressure infundibular compartment (Alva et al. 1999; Galal et al. 2000; Restivo et al. 1984; Said et al. 2012). In the majority of cases (75–80 %), double-chambered right ventricle occurs in association with perimembranous ventricular septal defects (Bashore 2007; Said et al. 2012). Ventricular septal defects in this setting are frequently restrictive and may close spontaneously. The presence of non-obstructive anomalous muscle bundles can be detected by echocardiography in early infancy, before they cause significant obstruction. Progressive hypertrophy of these preformed structures results

in an increasing pressure gradient within the cavity of the right ventricle. Furthermore DCRV may be associated with fibromuscular subaortic stenosis (Baumstark et al. 1978; Vogel et al. 1988).

Stenoses of the pulmonary bifurcation and of the central and peripheral pulmonary arteries are much less frequent than obstructions at valvular level. Stenoses of the pulmonary bifurcation at the origin of the left pulmonary artery are frequently due to constriction of ductal tissue at its pulmonary insertion. Therefore this type of obstruction has been termed juxtaductal pulmonary artery coarctation (Elzenga et al. 1990; Luhmer and Ziemer 1993; Momma et al. 1986). It is quite common in patients with complex cyanotic heart disease including tetralogy of Fallot or pulmonary atresia and VSD with duct-dependent pulmonary circulation (Elzenga et al. 1990; Luhmer and Ziemer 1993; Momma et al. 1986). In patients with right-sided duct connecting to the right pulmonary artery, the obstruction can be located at the origin of the right pulmonary artery. Juxtaductal pulmonary artery coarctation may progress to atresia, resulting in isolation of the respective pulmonary artery (Elzenga et al. 1990; Luhmer and Ziemer 1993; Momma et al. 1986).

Stenoses of the peripheral pulmonary arteries, frequently associated with hypoplasia of both central pulmonary arteries, are a typical feature of patients with Williams-Beuren syndrome (Pankau et al. 2001; Wessel et al. 1994). Further cardiovascular manifestations of this syndrome include supravalvular aortic stenosis, coarctation of the aorta and hypoplasia of the descending aorta (Collins 2013; Zalzstein et al. 1991). The syndrome, which is caused by a microdeletion on chromosome 7q22, includes a typical facial appearance ("elfin facies") and varying degrees of mental retardation (Collins 2013; Wessel et al. 1994). Similar cardiovascular manifestations in non-syndromic patients are caused by mutations of the *elastin* gene, which is localized within the area of microdeletion that is affected in patients with Williams-Beuren syndrome (Koch et al. 2003; Metcalfe et al. 2000). Peripheral pulmonary artery stenoses may also complicate Alagille syndrome (arteriohepatic dysplasia) which has been linked to mutations in *Jag1* and *Notch2* (Turnpenny and Ellard 2012). However in these children, it is frequently the hepatic pathology that dominates the clinical appearance of the disease.

True stenoses of the pulmonary artery bifurcation have to be differentiated from physiologic narrowing ("stenosis") of the bifurcation in preterm and term neonates (Chatelain et al. 1993;So et al. 1996). Newborns with physiologic stenosis of bifurcation are characterized by a mismatch between relatively large pulmonary trunks connected to relatively small but otherwise morphologically normal central pulmonary arteries. This results in a step up of flow velocities in the branch pulmonary arteries and a functional murmur, which usually resolves until the age of 5–6 months (Chatelain et al. 1993;So et al. 1996).

Although pulmonary regurgitation may be encountered as a primary malformation usually in combination with pulmonary stenosis, in the majority of patients, it will be the result of therapeutic efforts, to abolish significant valvular stenosis (Bove et al. 2012; 2012; Chaowalit et al. 2012). This refers primarily to surgical procedures, especially those requiring transannular patch enlargement of the main pulmonary artery. The majority of these patients had prior surgical repair of tetralogy of Fallot or DORV with pulmonary stenosis (Brown et al. 2012). Less commonly significant pulmonary regurgitation may also result from balloon dilatation of the pulmonary valve. Pulmonary regurgitation results in a volume load of the right ventricle with consecutive dilatation and reduced function of this chamber, necessitating pulmonary valve replacement in the long-term follow-up (Brown et al. 2012; Chaowalit et al. 2012; Eicken et al. 2011).

7.2 2D Echocardiography

Depending on the severity of pulmonary valvular stenosis, the apical four-chamber view demonstrates varying degrees of right ventricular hypertrophy (Fig. 7.2, Videos 7.1 and 7.2). In older children with mild to moderate stenosis, the right chamber may appear almost normal. In neonates however with critical stenosis, the right ventricle shows severe hypertrophy with attenuation of its apical component (Video 7.1). Assessment of the right ventricle should include evaluation of its function and measurement of tricuspid valve annulus. Critical pulmonary stenosis is associated with systemic or suprasystemic right ventricular pressure resulting in bulging of the ventricular septum from right to left. This can be recognized in the parasternal long and short axis (Fig. 7.3). The parasternal long and short axis view of the right ventricular outflow tract is the best plane to visualize the pulmonary valve and to determine the mechanism of obstruction (Fig. 7.4, Videos 7.3, 7.4 and 7.5). In pulmonary valvular stenosis, the leaflets are thickened and show restricted separation (so-called doming). In critical stenosis, even frame-by-frame analysis of the pulmonary valve leaflets may not provide sufficient information to distinguish severe stenosis from complete valvular atresia without the help of colour Doppler. In neonates with critical stenosis, the degree of thickening of the valve leaflets may be quite pronounced, making it difficult to distinguish patients with stenosis due to commissural fusion from patients with truly dysplastic valves (Fig. 7.5). The latter however frequently show absence of dilatation of the sinuses of Valsalva in diastole and some additional narrowing at the level of the sinotubular junction (Musewe et al. 1987) (Videos 7.6 and 7.7).

Evaluation of the valve includes measurement of its diameter at the ventriculoarterial junction (so-called annulus) as

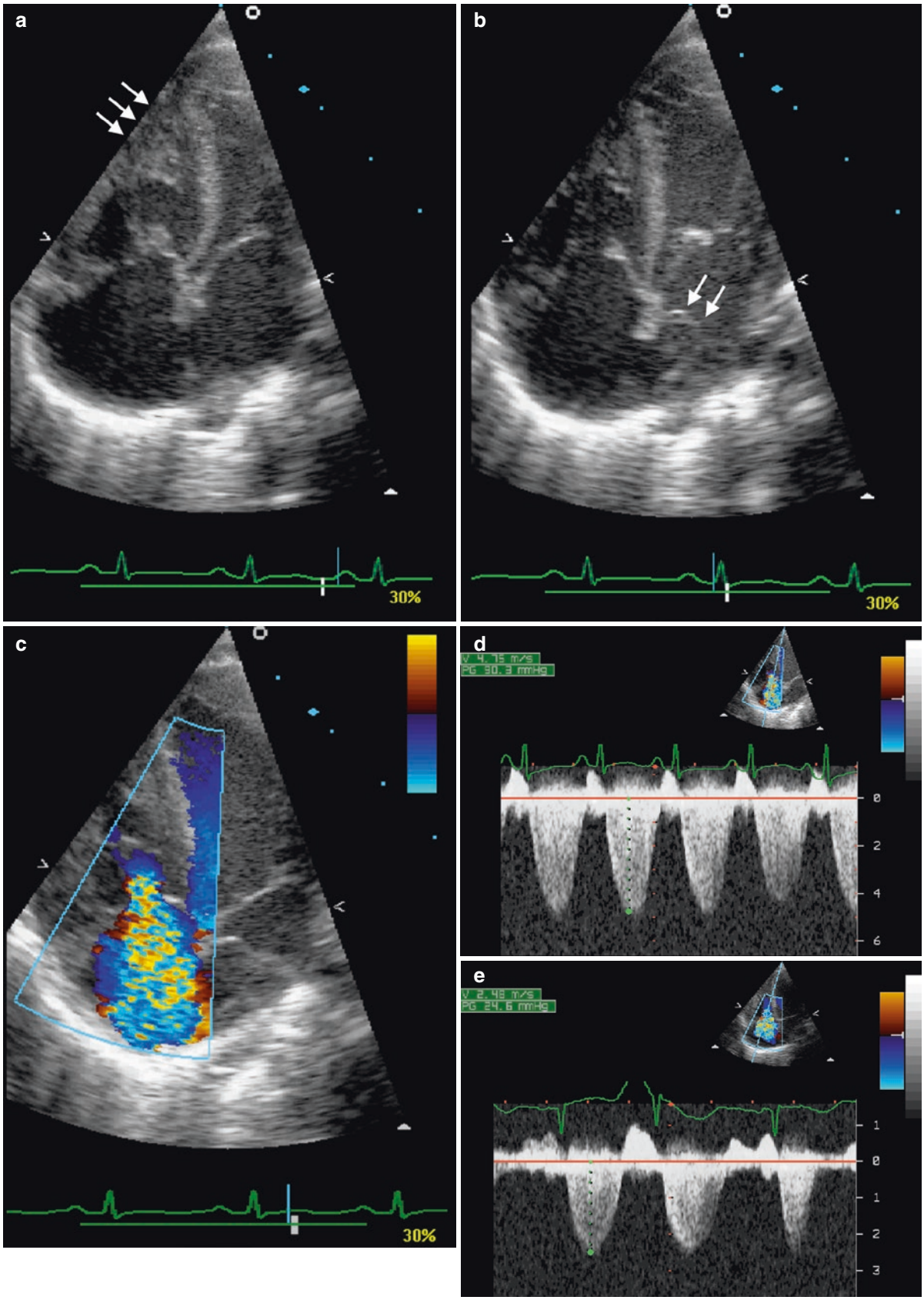

Fig. 7.2 Apical four-chamber view in a neonate with critical pulmonary stenosis with significant apical hypertrophy (arrows) of the right ventricle (**a**). The diastolic frame shows bulging (*arrows*) of the atrial septum from right to left (**b**). Severe tricuspid regurgitation is displayed by colour Doppler (**c**) with a maximal velocity of 4,75 m/s on CW Doppler documenting suprasystemic right ventricular pressure (**d**). Following balloon valvuloplasty, the gradient of tricuspid regurgitation decreases to 2,48 m/s corresponding to a gradient of 24,6 mmHg (**e**)

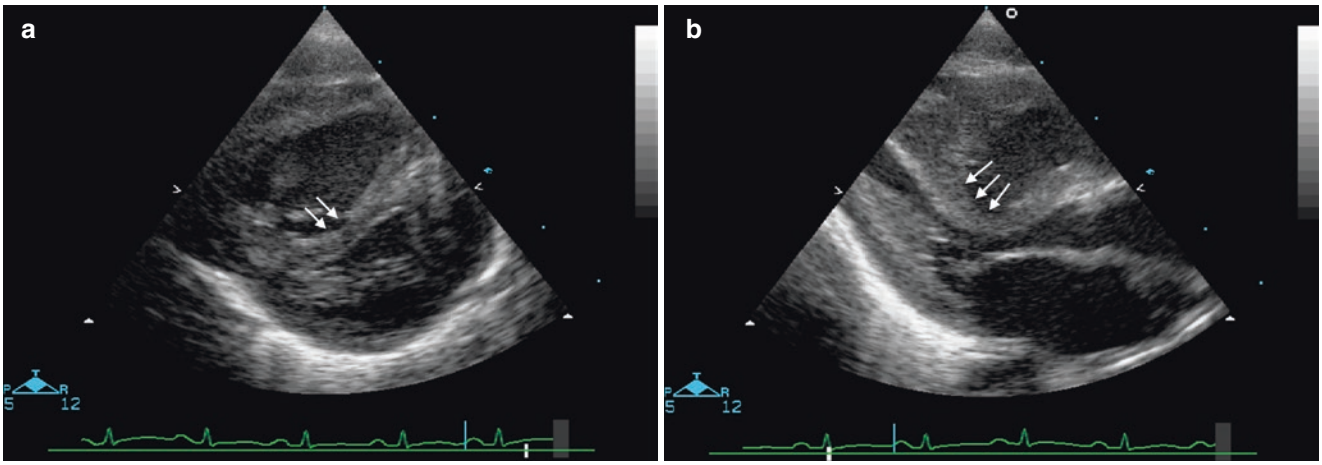

Fig. 7.3 Parasternal short axis view in a neonate with critical pulmonary stenosis and suprasystemic right ventricular pressure shows bulging (*arrows*) of the ventricular septum from right to left (**a**). Bulging is even more apparent (*arrows*) in the parasternal long axis (**b**)

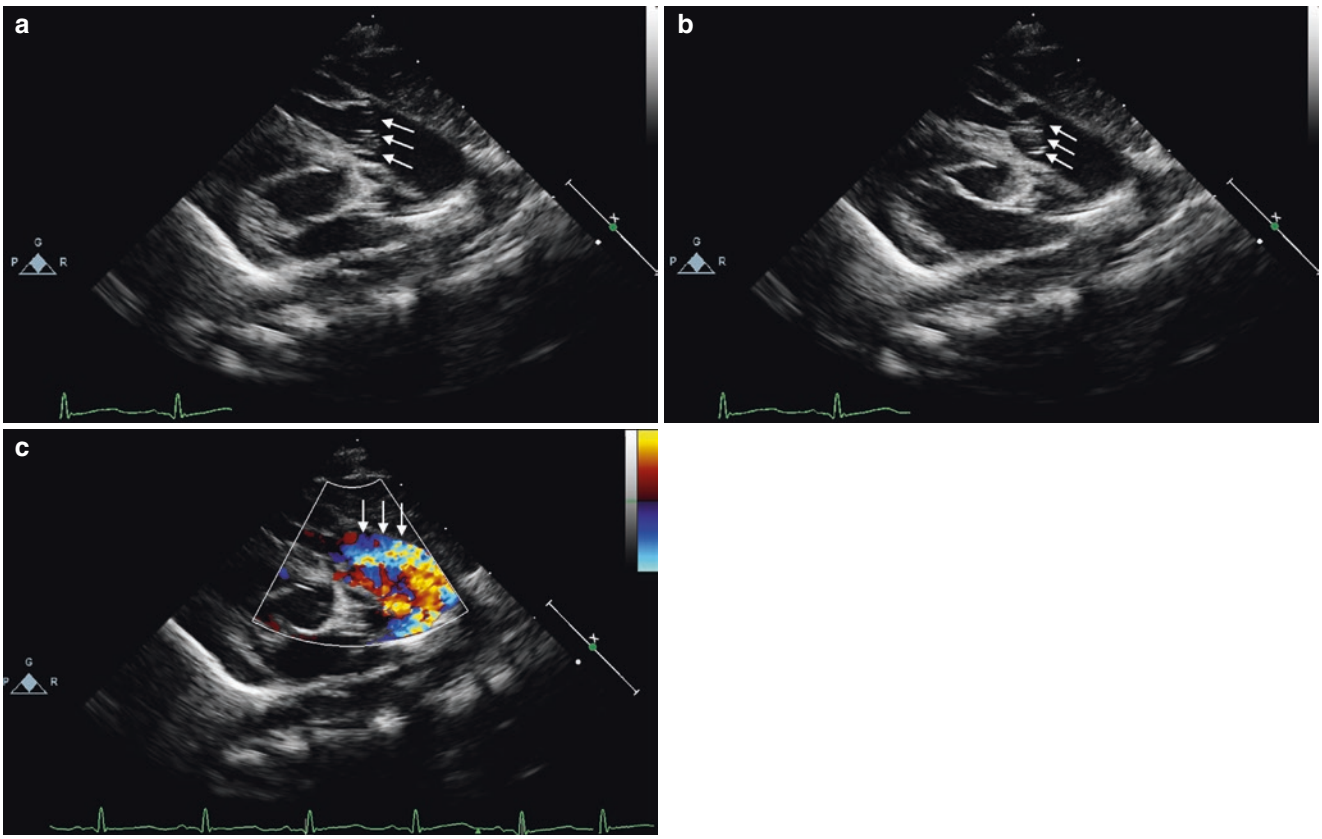

Fig. 7.4 Parasternal long axis view of the right ventricular outflow tract in neonatal severe pulmonary valve stenosis shows limited separation (doming) of the valve (*arrows*) in systole (**a**). Thickening of the valve is even more apparent in diastole (**b**). Colour Doppler displays an eccentric jet (*arrows*) directed towards the lateral wall of the main pulmonary artery (**c**)

well as measurement of the diameter of the sinotubular junction. Both measurements are relevant for planning interventional balloon valvuloplasty. Children with valvular stenosis frequently show poststenotic dilatation of the main pulmonary artery, which is absent in patients with subvalvular obstruction (Fig. 7.6). The degree of poststenotic dilatation does not correlate with the severity of valvular obstruction: quite severe dilatation of the main pulmonary artery may be present even in very mild forms of valvular stenosis.

Direct visualization of the pulmonary valve in cross section is possible in neonates and infants from a left parasternal window with 90^0 rotation of the transducer from the parasternal long axis view of the right ventricular outflow tract (Fig. 7.7, Videos 7.8 and 7.9) (Lemler and Ramaciotti 2009;

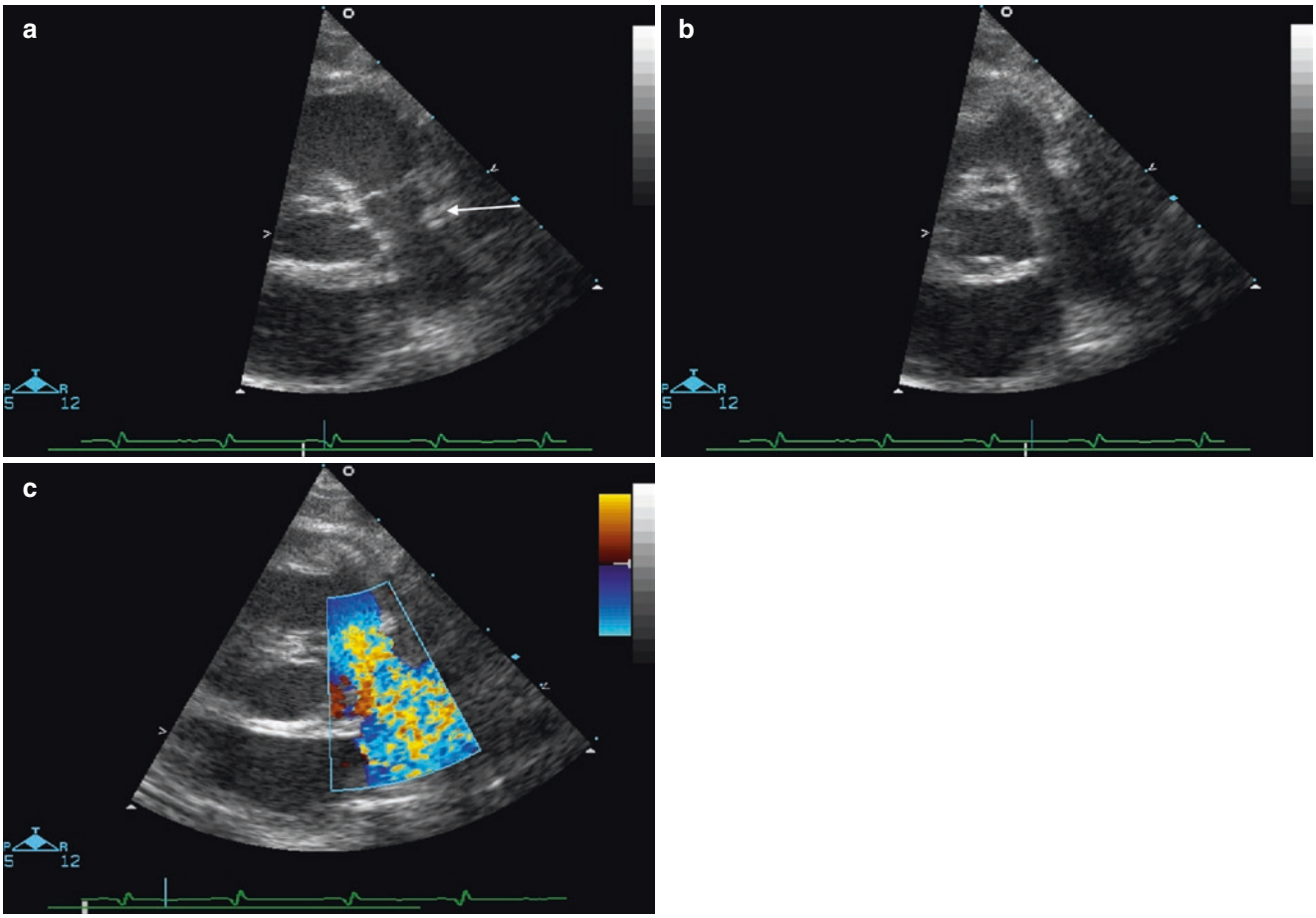

Fig. 7.5 In a patient with Noonan syndrome and dysplastic pulmonary valve, the parasternal short axis view shows mild narrowing (*arrow*) at the sinotubular junction in diastole (**a**). Although the valve does not appear dysplastic in the systolic frame (**b**), colour Doppler reveals significant valvular stenosis (**c**)

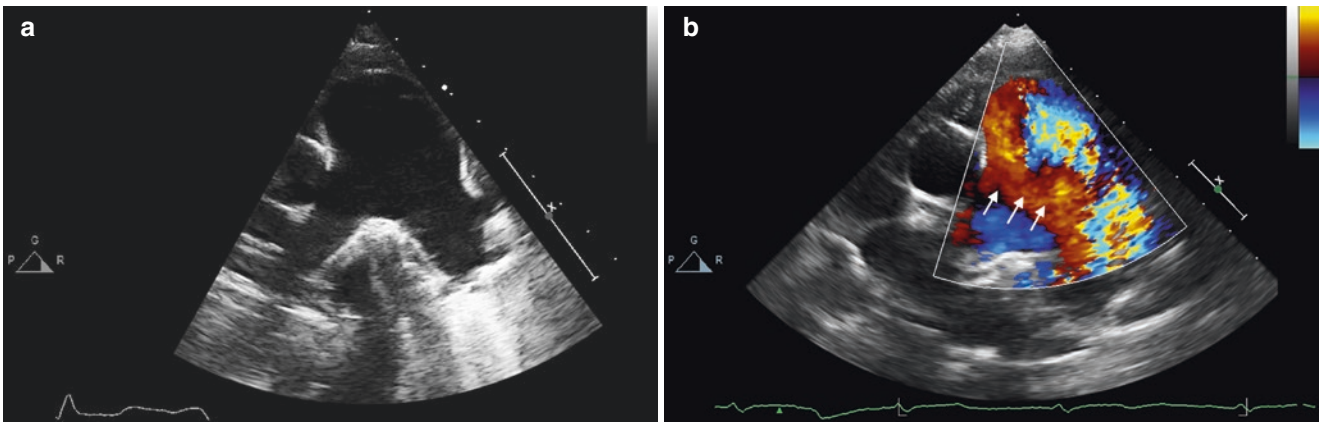

Fig. 7.6 Significant poststenotic dilatation of the main pulmonary artery (parasternal short axis view) in a child with mild pulmonary valve stenosis (**a**). Colour Doppler shows turbulence (**b**) with some retrograde flow towards the medial aspect of the pulmonary artery (*arrows*)

Martinez and Anderson 2005; McAleer et al. 2001). The subcostal views provide additional options to display the right ventricle, the outflow tract, the pulmonary valve and the main pulmonary artery (Fig. 7.8).

Subvalvular stenosis can be detected in the parasternal short axis view as well. It may present either as infundibular narrowing or as abnormal muscle bundles proximal to the infundibulum (Fig. 7.9). Fixed infundibular stenosis has to be

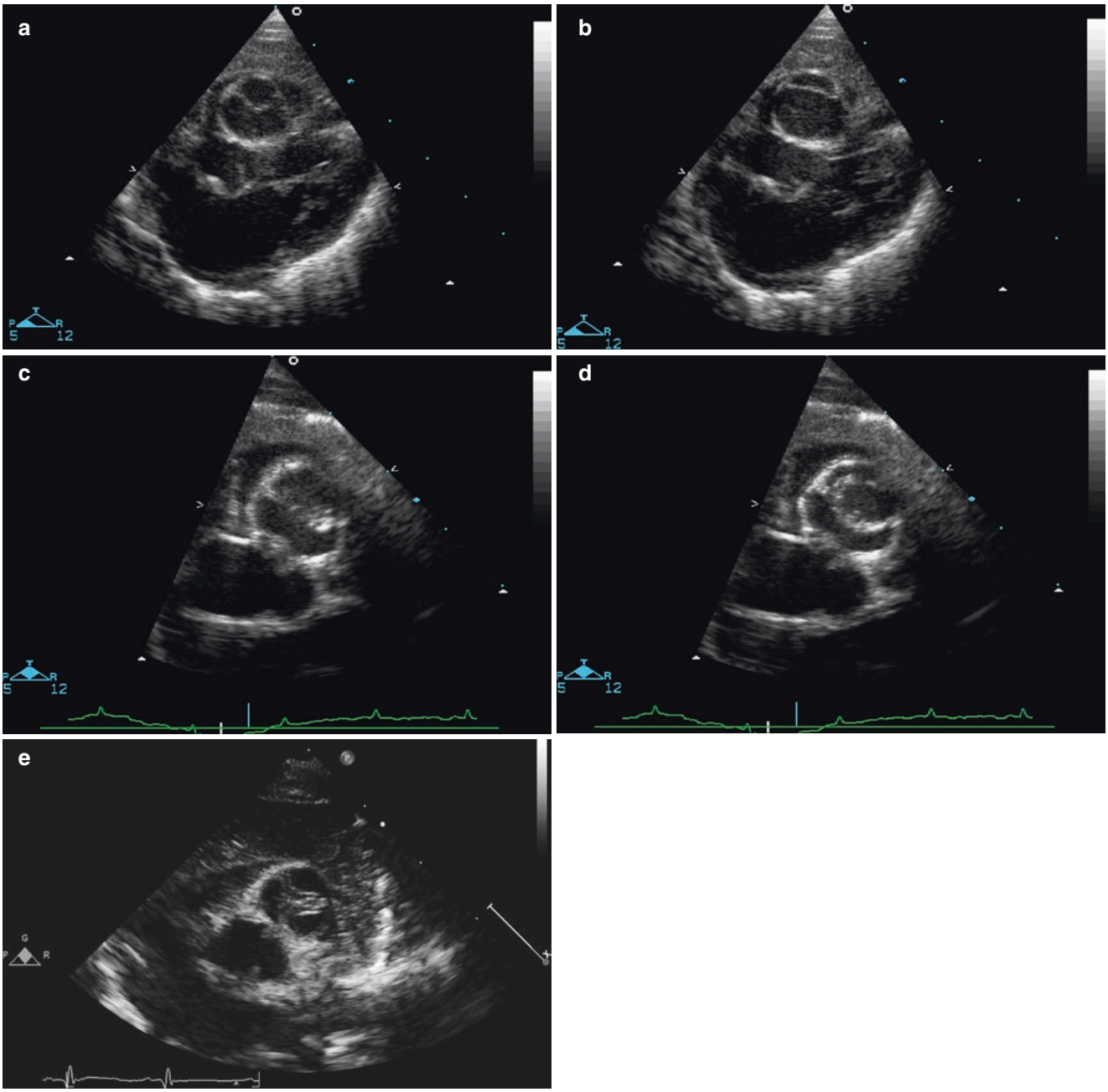

Fig. 7.7 Diastolic frame (**a**) of the normal tricuspid pulmonary valve in a neonate (high left parasternal short axis view); normal separation of the valve leaflets in systole (**b**). The stenotic bicuspid pulmonary valve of another neonate (**c**) shows incomplete separation during systole (**d**). Significant thickening of the valve leaflets is present in this neonate with critical stenosis and tricuspid pulmonary valve (**e**)

discriminated from reactive infundibular narrowing, which is frequently present in patients with severe valvular stenosis. The latter demonstrates significant widening of the infundibulum up to a normal diameter during diastole, while the former exhibits some narrowing during the entire cardiac cycle. Anomalous muscle bundles can be detected in the parasternal short axis encroaching onto the lumen of the right ventricle (Fig. 7.9, Videos 7.10 and 7.11). In infants the subcostal planes are extremely helpful to verify double-chambered right ventricle (Martinez and Anderson 2005). The obstruction by abnormal muscle bundles proximal to the infundibulum can be well exhibited in the subcostal coronal and sagittal and RAO views of the right ventricular outflow tract (Fig. 7.10, Video 7.12).

Supravalvular stenoses are best visualized in the parasternal short axis views. This applies specifically to the so-called juxtaductal pulmonary artery coarctation, developing due to constriction of ductal tissue at the pulmonary end of the ductus

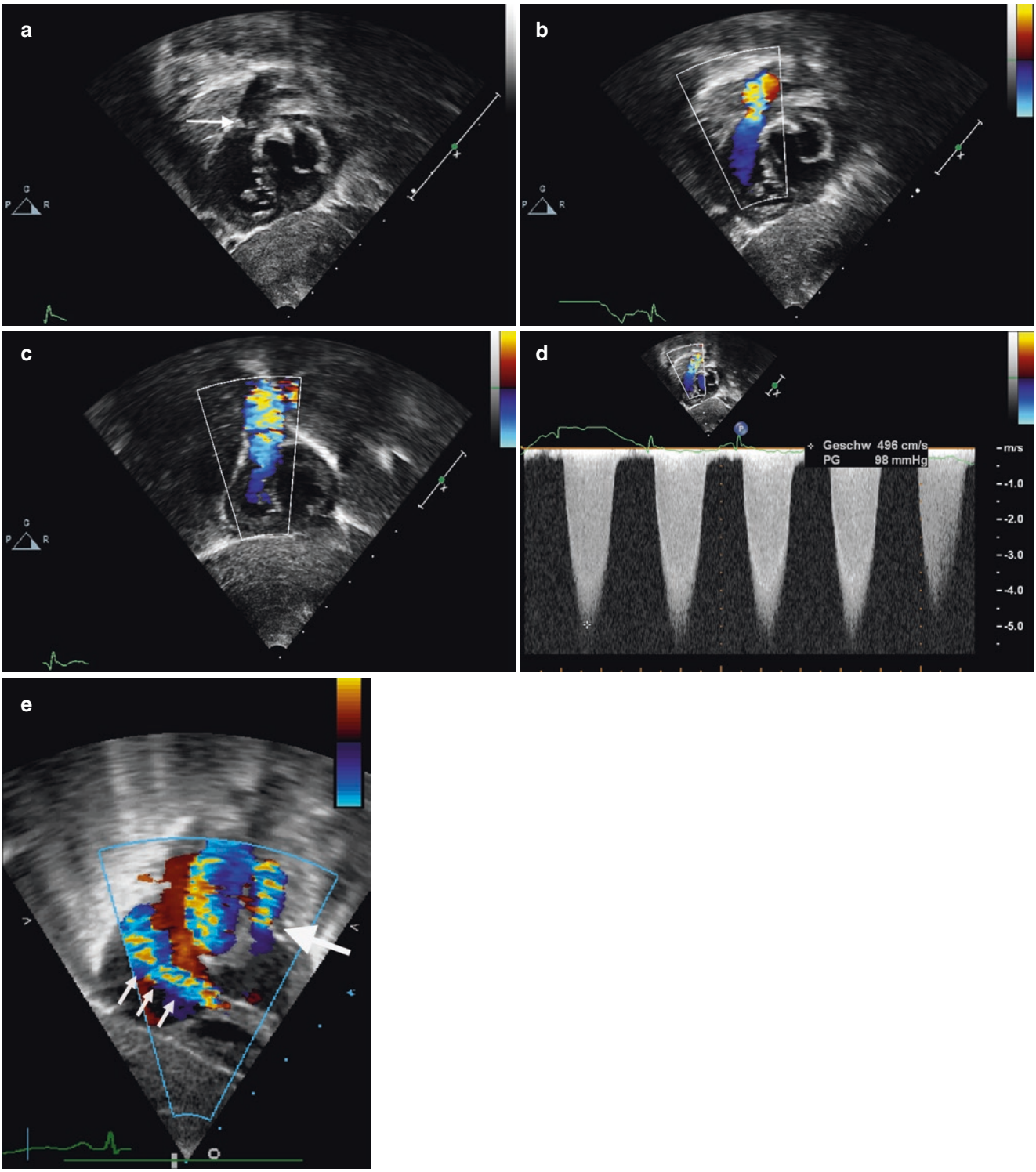

Fig. 7.8 Thickening (*arrow*) of the valve leaflets (subcostal short axis of the right ventricular outflow) in a neonate with severe pulmonary stenosis (**a**). Colour Doppler in the short axis (**b**) and in the coronal view shows acceleration of flow starting at valvular level (**c**). CW Doppler reveals a maximal flow velocity of 4,96 m/s corresponding to a peak instantaneous gradient of 98 mmHg (**d**). Colour Doppler in the subcostal RAO view of a neonate with critical pulmonary stenosis shows both the obstruction at valvular level (*arrow*) and tricuspid regurgitation (*small arrows*) (**e**)

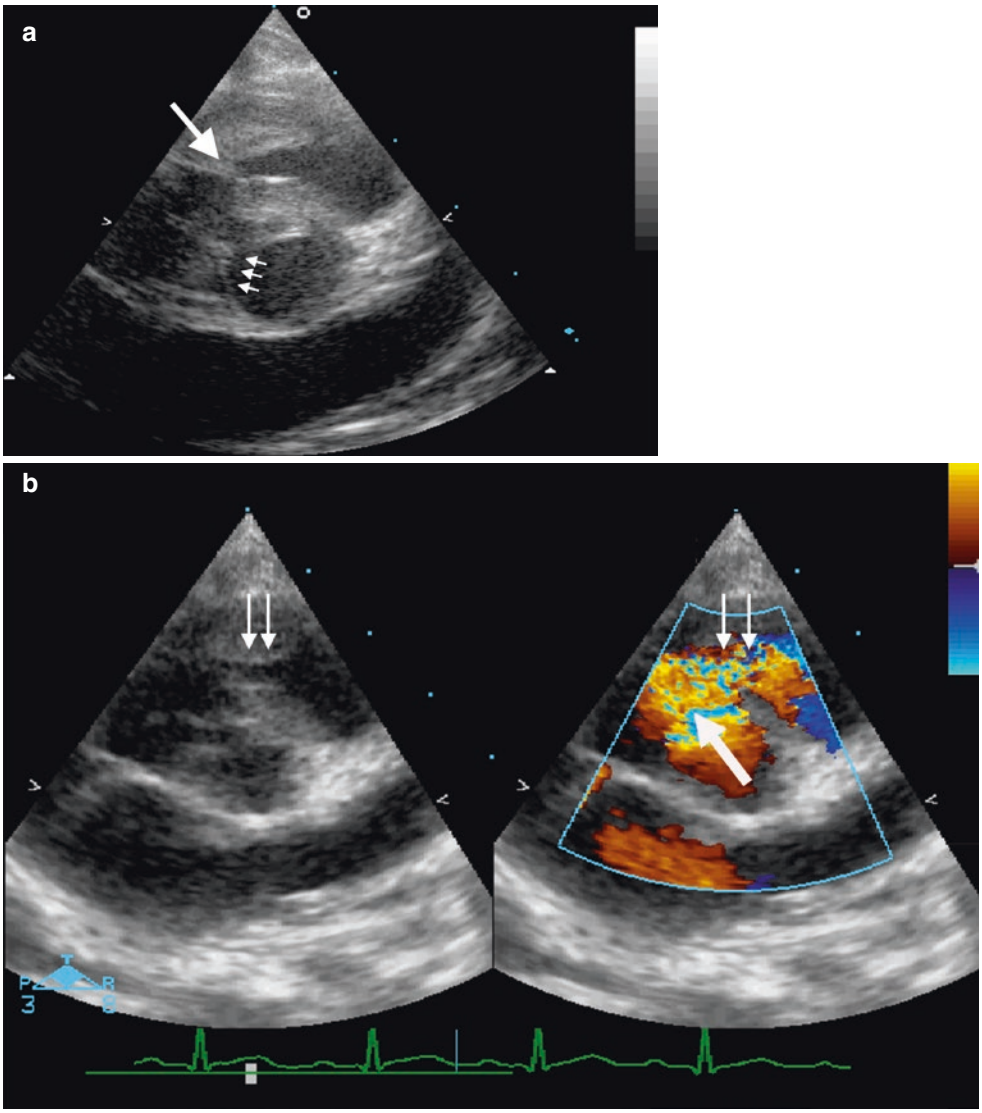

Fig. 7.9 Parasternal short axis view (**a**) depicting anomalous muscle bundles (*large arrow*) in a child with double-chambered right ventricle and perimembranous VSD, partially occluded by tricuspid valve tissue (*small arrows*). Colour Doppler reveals both acceleration of flow due to the muscle bundles (*arrows*) and LR-shunting (*large arrow*) across the VSD (**b**)

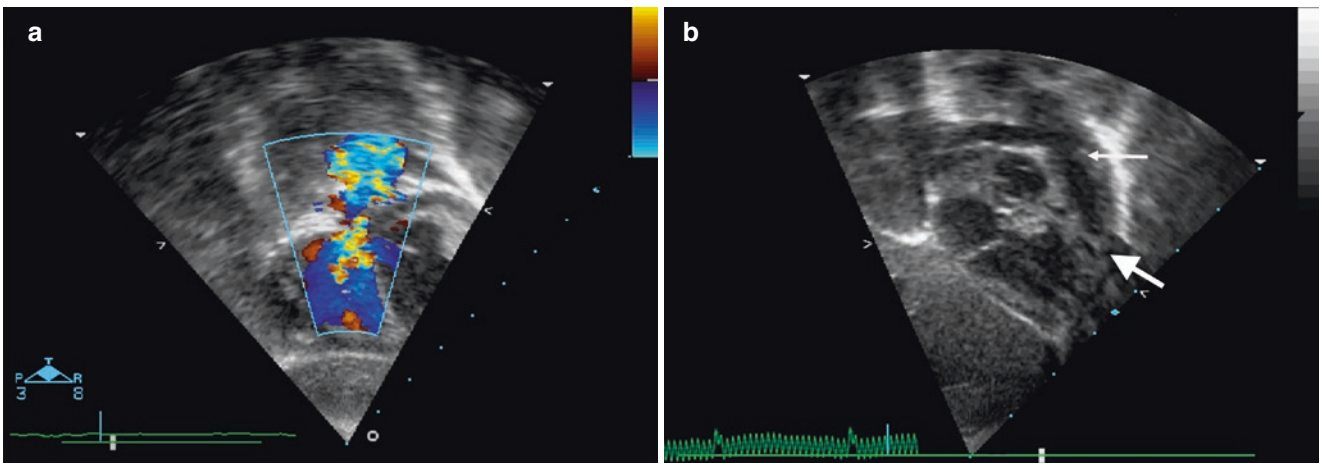

Fig. 7.10 Colour Doppler in the subcostal coronal view shows significant obstruction due to anomalous muscle bundles well below the pulmonary valve in this child with DCRV (**a**). The distance between the muscle bundles (*large arrow*) and the pulmonary valve (*small arrow*) is well displayed in the subcostal RAO view (**b**)

arteriosus (Elzenga et al. 1990; Luhmer and Ziemer 1993; Momma et al. 1986). It is frequently possible to detect a fibrous shelf in continuation with the pulmonary insertion of the ductus arteriosus at the origin of the left pulmonary artery (Fig. 7.11, Video 7.13). Furthermore stenoses at the origin of the left pulmonary artery can be well displayed in the ductal view (Fig. 7.12). In addition this plane offers a reasonable angle for Doppler interrogation of the left pulmonary artery.

Patients with Williams-Beuren syndrome or Allagille syndrome frequently present with global hypoplasia of both central pulmonary arteries in association with central or peripheral pulmonary artery stenoses. The main pulmonary artery may be of normal size with a significant reduction in calibre of both central pulmonary arteries beginning at their origin from the bifurcation (Fig. 7.13, Video 7.14). The description of stenoses beyond the bifurcation requires other imaging modalities like CT thorax, cardiac MRI or cardiac catheterization and angiography (Grosse-Wortmann and Yoo 2010).

In newborns with physiologic stenosis of the bifurcation, careful visualization of the origin of the right and left pulmonary artery by 2D echo is important to discriminate them from patients with anatomical obstruction (Fig 7.14). Further differentiation is possible by the application of pulsed wave and continuous wave Doppler (Chatelain et al. 1993; So et al. 1996): flow velocities in neonates with physiologic narrowing of the bifurcation usually do not exceed 2,5 m/s and normalize until the age of 6 months.

7.3 Colour Doppler Echocardiography

In the evaluation of patients with pulmonary valvular stenosis, colour Doppler echocardiography helps to clarify several important issues: *it allows confirmation of patency of the valve*, *determination of additional subvalvular obstruction and visualization of the direction of the jet*. While patients with critical pulmonary stenosis present a high velocity jet from the right ventricle entering the main pulmonary artery, there is only retrograde flow from the ductus arteriosus in patients with pulmonary atresia (Fig. 7.4). Colour Doppler interrogation of the pulmonary valve and the right ventricular outflow tract can be performed in the parasternal short axis, in the parasternal long axis of the right ventricular outflow tract and in the subcostal views (Fig. 7.4 and 7.8, Videos 7.4, 7.5 and 7.15). Subvalvular obstruction can be suspected, if acceleration of flow is noted below the plane of the valve (Fig. 7.10). Colour Doppler allows visualization of the jet, which is important in patients with eccentric jets (Fig. 7.4) to adjust the plane of PW and CW Doppler interrogation for quantification of the Doppler gradient and to avoid underestimation of its velocity.

Detection and semiquantitative gradation of severity of pulmonary regurgitation is a domain of colour Doppler echocardiography. Minor amounts of pulmonary regurgitation are frequently found in normal children and do not represent a pathologic finding (Fig. 7.15, Video 7.16). They have been described in 17 % of normal infants (Lee and Lin 2010). The incidence is even higher in the adult population with 40–78 % (Lancellotti et al. 2010). Quantification of pathologic pulmonary regurgitation is based on width and length of the jet (Lancellotti et al. 2013; Puchalski et al. 2008). A jet width occupying >50–65 % of the right ventricular outflow tract suggests severe pulmonary regurgitation (Lancellotti et al. 2013; Puchalski et al. 2008) (Video 7.17). Despite numerous attempts to establish objective parameters, quantification of pulmonary regurgitation by colour Doppler remains semiquantitative and should be interpreted with caution. Detection of reversal colour Doppler flow in the pulmonary arteries (Fig. 7.15, Video 7.18) however is very specific for severe pulmonary regurgitations (Lancellotti et al. 2013; Puchalski et al. 2008).

In the presence of central pulmonary artery stenoses, colour Doppler examination of the pulmonary bifurcation in the parasternal short axis view reveals acceleration of flow and turbulence in the branch pulmonary arteries (Figs. 7.11, 7.12 and 7.13). Neonates with critical pulmonary valvular stenosis are dependent on collateral blood flow from the ductus arteriosus. Therefore the bifurcation should be screened carefully for evidence of LR-shunting via a patent ductus arteriosus (Fig. 7.11). Examination of the aortic arch from the suprasternal notch or from the right parasternal window demonstrates the ductus originating from the undersurface of the arch with continuous left to right shunting (see Chap. 8).

Colour Doppler interrogation of the tricuspid valve should be performed to detect tricuspid regurgitation and to determine its severity by estimation of length and width of the regurgitant jet (Fig. 7.2, Video 7.2). Exact delineation of the jet is a prerequisite for PW and CW Doppler interrogation for noninvasive determination of RV pressure.

Neonates with severe pulmonary valvular stenosis almost always have an interatrial communication. In the majority of cases, this will be a patent foramen ovale. Colour Doppler interrogation of shunting across the foramen ovale provides valuable haemodynamic information in the neonate: patients with critical pulmonary stenosis initially present RL-shunting across the atrial septum (Fig. 7.16). Following successful balloon dilatation, RL-shunting may persist for days or even weeks, due to increased stiffness of the hypertrophied right ventricle, until it gradually converts into LR- shunting.

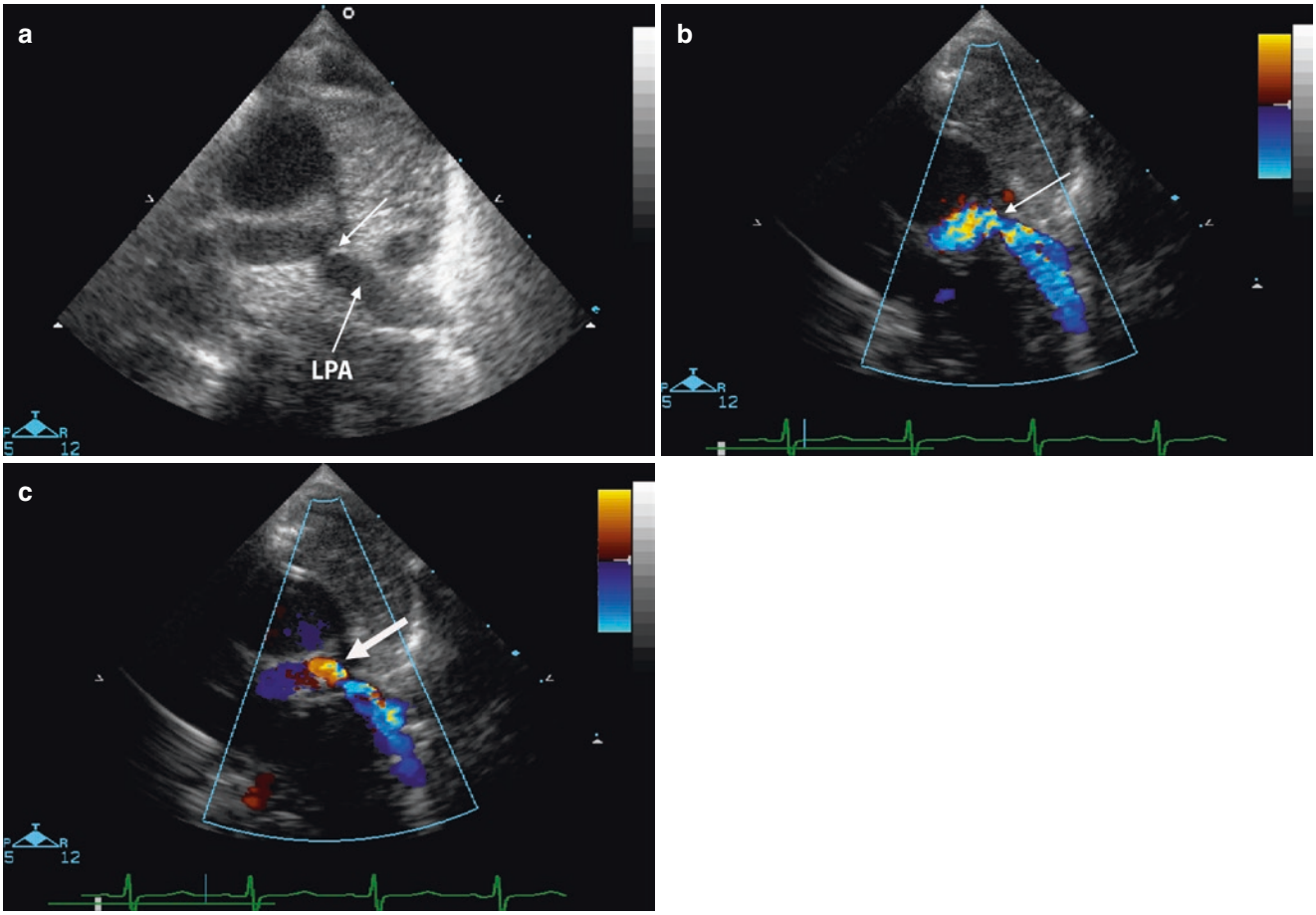

Fig. 7.11 Fibrous shelf (*arrow*) at the pulmonary insertion of the ductus arteriosus obstructing the left pulmonary artery (*LPA*) in the parasternal short axis view (**a**). Colour Doppler in systole (**b**) confirms the narrowing (*arrow*), and the diastolic frame (**c**) shows residual shunting (*arrow*) via the ductus arteriosus

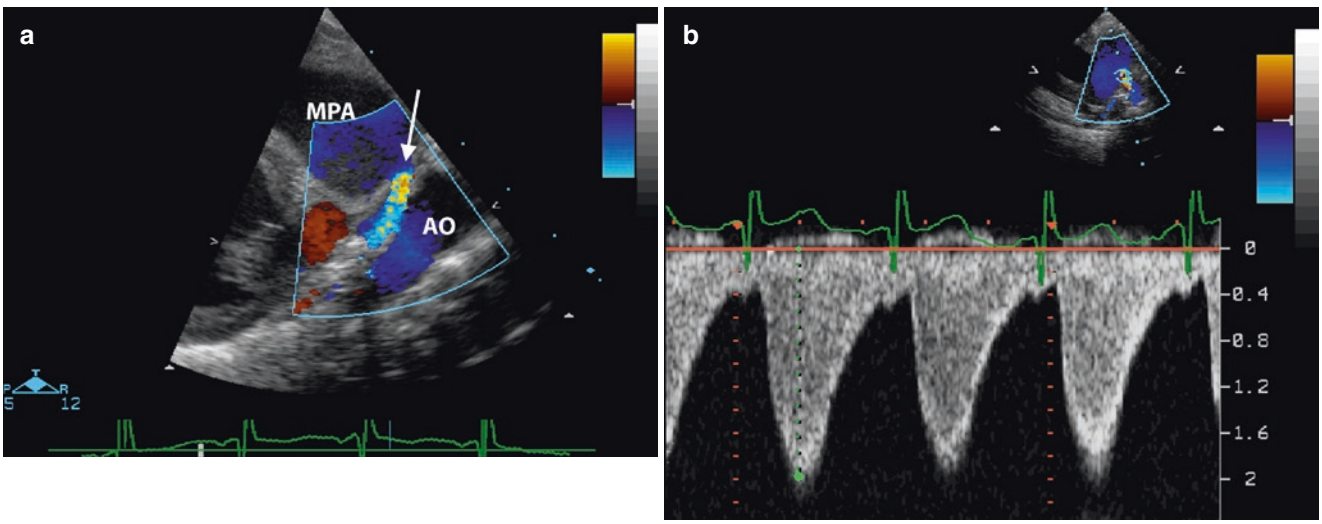

Fig. 7.12 Colour Doppler in the ductal view (**a**) shows severe stenosis of the left pulmonary artery (*arrow*). Pulsed wave Doppler (**b**) reveals acceleration and turbulent flow in systole and in diastole. *MPA* main pulmonary artery, *AO* descending aorta

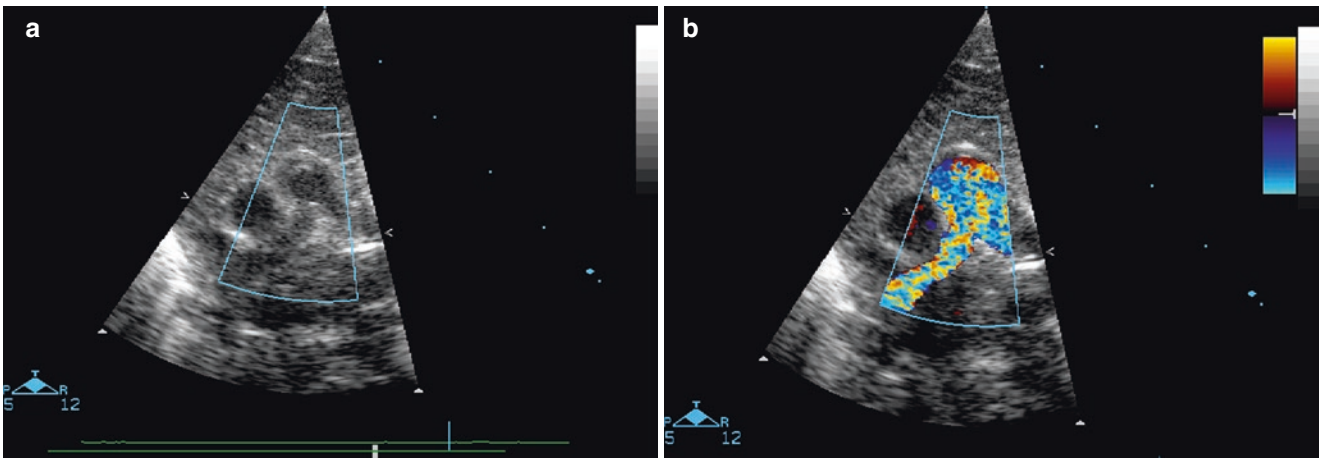

Fig. 7.13 Parasternal short axis view of an infant with Williams-Beuren syndrome demonstrating diffuse stenosis both of the right and of the left pulmonary arteries (**a**). Colour Doppler confirms acceleration of flow in the main and right pulmonary artery (**b**)

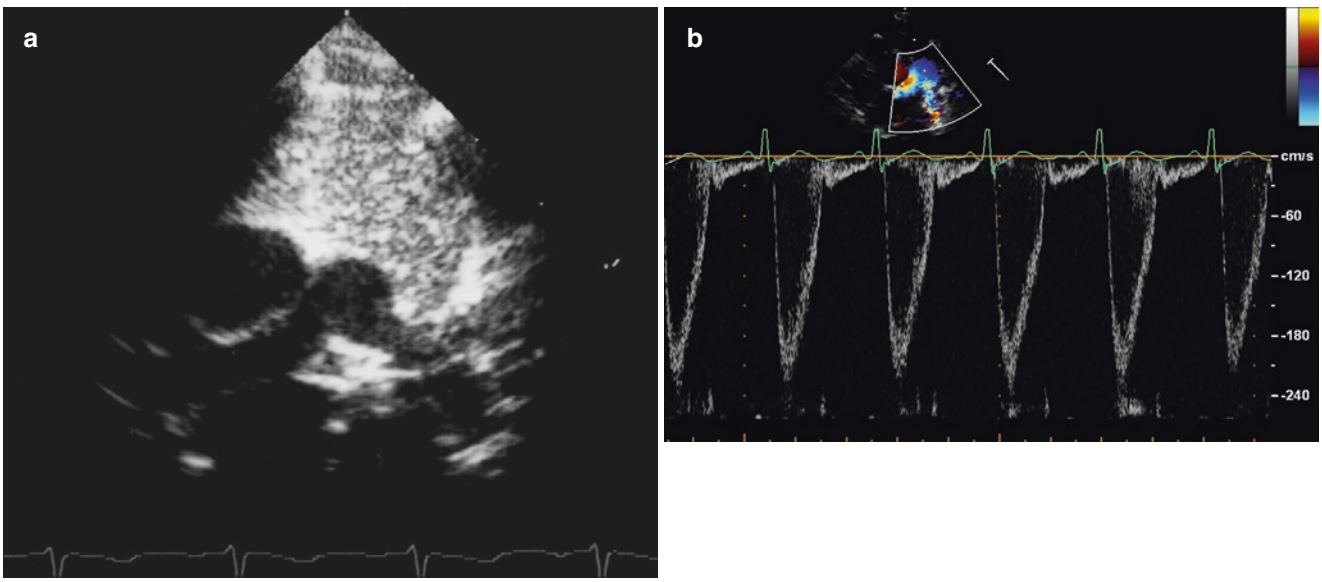

Fig. 7.14 No circumscript narrowing is apparent in the parasternal short axis view of a newborn with physiological pulmonary branch stenosis (**a**). Pulsed wave Doppler in the left pulmonary artery shows a maximal velocity of 2 m/s (**b**)

7.4 Pulsed Wave and Continuous Wave Doppler

Doppler evaluation in patients with pulmonary stenosis aims to determine the peak instantaneous gradient between the right ventricle and pulmonary artery and to estimate right ventricular systolic pressure (Aldousany et al. 1989; Silvilairat et al. 2005a, b).

In patients with pulmonary valvular stenosis, interrogation of the jet across the valve, for determination of the pressure gradient, is best achieved in the parasternal short axis and in the parasternal long axis of the right ventricular outflow tract (Martinez and Anderson 2005). Colour Doppler is required to adjust the Doppler interrogation to the direction of the jet which may be quite eccentric (Fig. 7.4). Further planes for Doppler interrogation of the right ventricular outflow tract and the pulmonary valve are the subcostal short axis view of the right ventricular outflow tract and the subcostal RAO view (Martinez and Anderson 2005). *The subcostal planes are especially useful in the Doppler interrogation of subvalvular obstructions*. This refers specifically to patients with DCRV: in contrast to the precordial

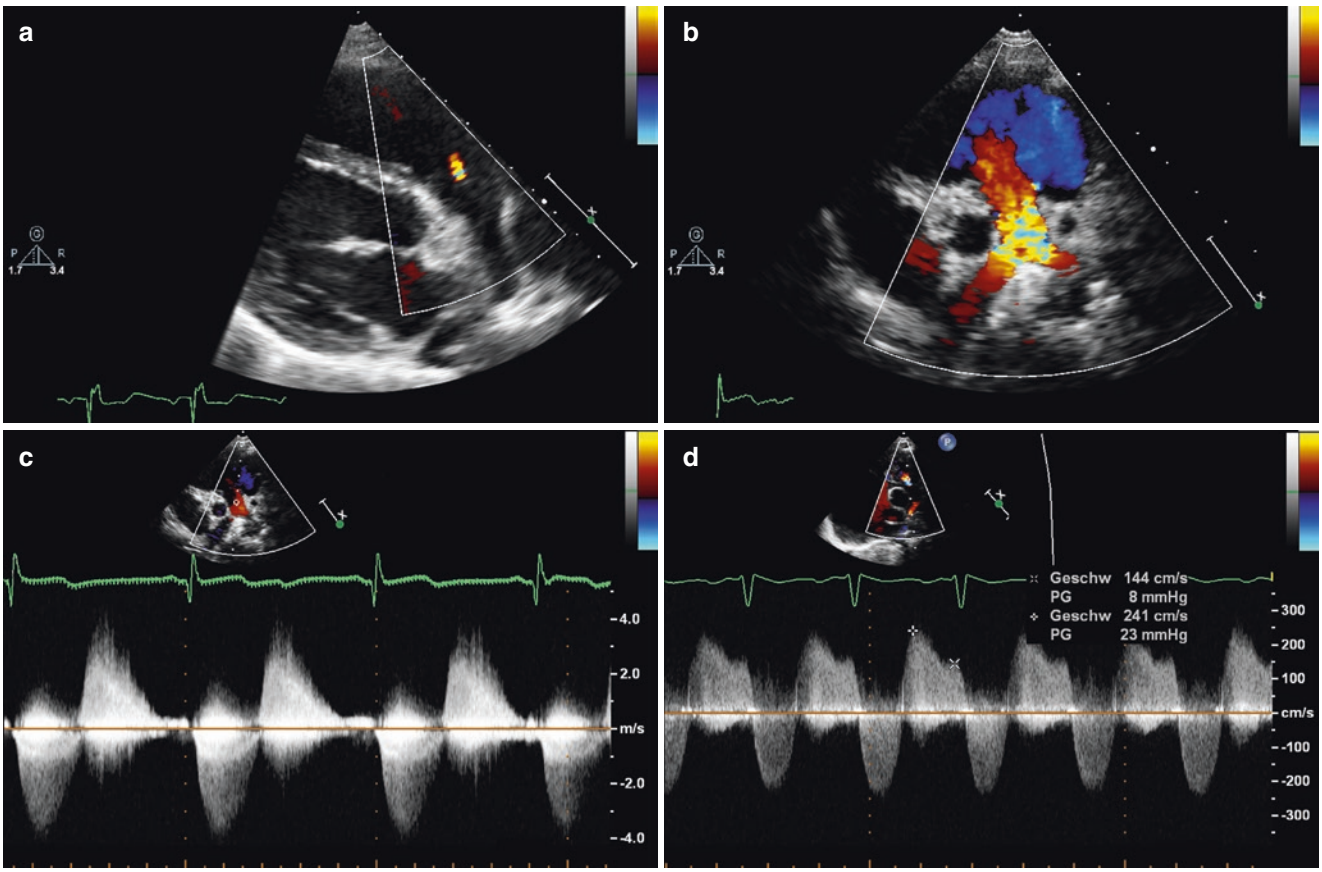

Fig. 7.15 Minor amount of physiological pulmonary regurgitation (parasternal long axis of the right ventricular outflow tract) in a 4-year-old child (**a**). Reverse flow in the main pulmonary artery and pulmonary bifurcation (parasternal short axis view) in a 3-year-old child with severe pulmonary regurgitation (**b**). Due to obstruction of both pulmonary arteries at the bifurcation, continuous wave Doppler shows acceleration of flow in systole and significant regurgitation characterized by rapid decrease of flow velocity in diastole (**c**). Continuous wave Doppler in a neonate shows pulmonary regurgitation with a maximal diastolic velocity of 2.41 m/s. The diastolic gradient of 23 mmHg in the presence of a central venous pressure of 10 mmHg indicated elevated mean pulmonary pressure of 33 mmHg confirmed by cardiac catheterization (**d**)

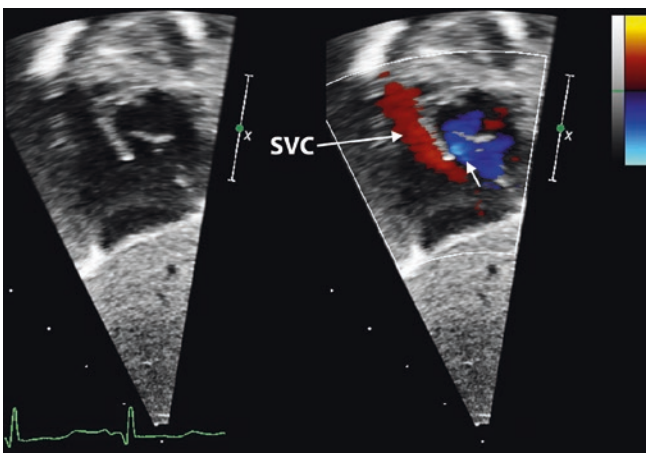

Fig. 7.16 Colour Doppler in the subcostal sagittal view of the right atrium in a neonate with critical pulmonary stenosis shows RL-shunting (*arrow*) across the foramen ovale. *SVC* superior vena cava

views, which offer an unfavourable angle for Doppler interrogation, there is good alignment of the Doppler beam with the jet in the subcostal views (Fig. 7.10). The peak instantaneous gradient across the right ventricular outflow tract is calculated according to the simplified Bernoulli equation. It has been recommended, however, to determine the mean pressure gradient as well, since the peak instantaneous gradient tends to be 25–40 % higher as compared to the invasively measured peak to peak gradient during cardiac catheterization (Aldousany et al. 1989; Silvilairat et al. 2005a, b).

In patients with subvalvular obstruction due to anomalous muscle bundles, colour Doppler is extremely important not to mistake the jet of the frequently associated VSD (Fig. 7.9) for the jet of outflow tract obstruction (Snider et al. 1997). Subvalvular obstructions of the right

ventricular outflow tract, associated with a dynamic muscular component, can be recognized by a specific Doppler flow pattern: it is characterized by a delayed but continuous increase of flow velocity during systole, as opposed to the rapid increase at the beginning of systole in patients with exclusive valvular obstruction (Fig. 7.17). In patients with combined subvalvular and valvular obstruction, CW Doppler may show superimposition of both flow signals (Fig. 7.17). This situation is frequently encountered in infants with tetralogy of Fallot (Chap. 11).

Estimation of right ventricular systolic pressure requires the presence of mild or moderate tricuspid regurgitation, which is quite common in patients with pulmonary stenosis (Fig. 7.2). Based on the velocity of the regurgitant jet, the systolic gradient between the right ventricle and the right atrium can be calculated based on the simplified Bernoulli equation. To obtain the systolic right ventricular pressure, an estimated (5 mmHg) or invasively measured right atrial pressure (e.g. by a central venous line) has to be added:

$$\text{Systolic pressure RV} = 4 \times \text{velocity tricuspid regurgitation}^2 + \text{mean pressure RA}$$

In the presence of relevant pulmonary stenosis, Doppler interrogation of the tricuspid regurgitant jet requires continuous wave Doppler, since the velocities will exceed the range of PW Doppler (Fig. 7.2).

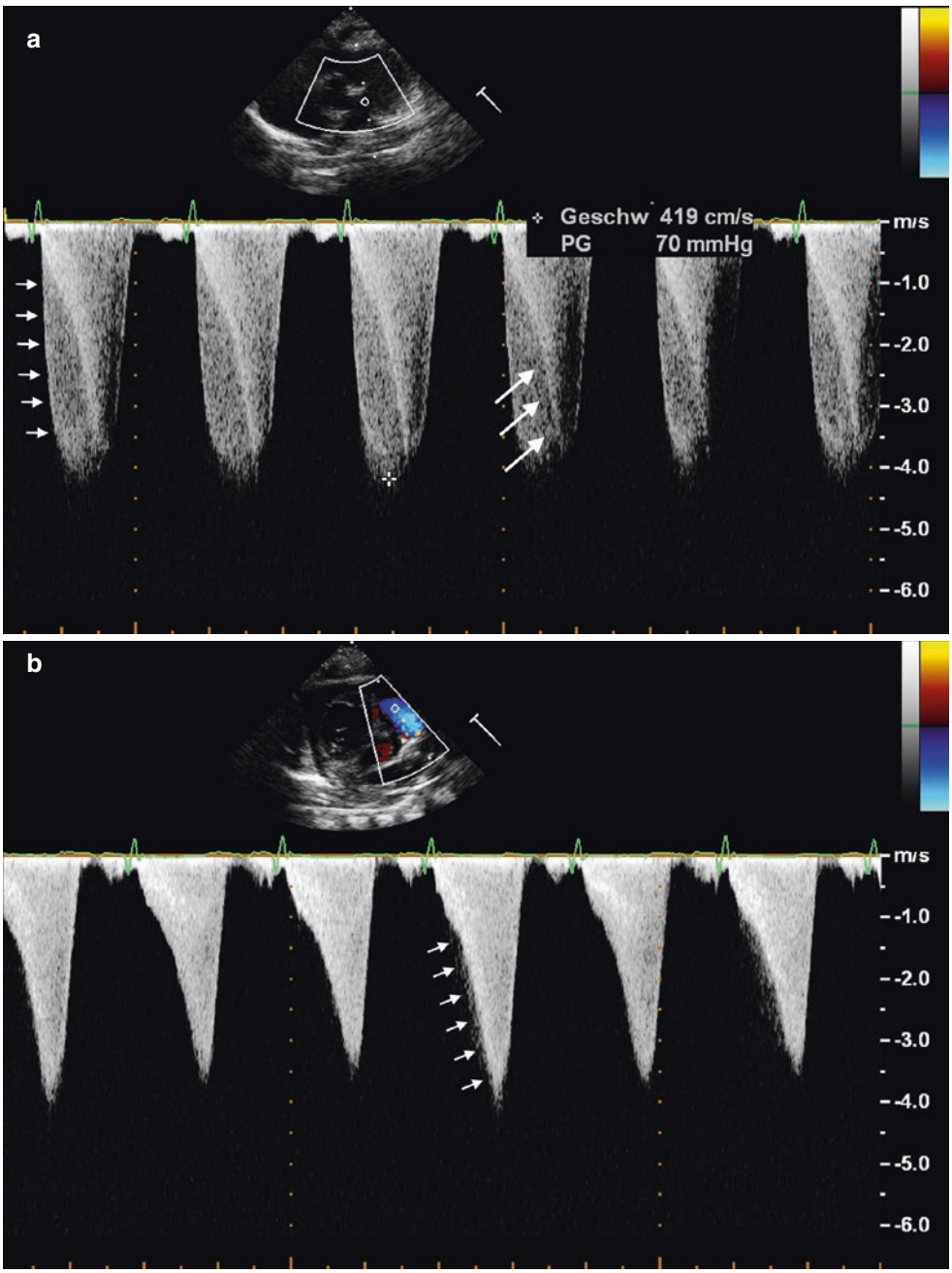

Fig. 7.17 Continuous wave Doppler interrogation of the right ventricular outflow tract in an infant with tetralogy of Fallot shows combined subvalvular and valvular pulmonary stenosis. In the parasternal short axis, flow velocity displays a rapid increase in systole (*small arrows*) due to severe valvular stenosis with a maximal flow velocity of 419 cm/s (**a**). The Doppler tracing contains a second superimposed flow curve (*large arrows*), which is displayed by choosing an insonation angle that depicts exclusive flow across the infundibulum (**b**). It is characterized by a slower, continuous increase in flow velocity (*arrows*), due to contraction and progressive narrowing of the infundibulum during systole

Lower gradients across the pulmonary valve may be encountered in neonates with critical pulmonary stenosis: they may present with low pressure gradients despite severe valvular obstruction. This can be explained by elevated pulmonary artery pressures due to neonatal elevation of pulmonary artery resistance. *Therefore assessment of the severity of pulmonary stenosis in neonates cannot rely exclusively on the pressure gradient but has to include other factors including right ventricular size, hypertrophy and function as well as morphology of the valve, flow across the valve and patency of the ductus arteriosus*.

Pulmonary regurgitation can be well documented by pulsed wave or continuous wave Doppler (Fig. 3.15). However there is no clinically accepted method of quantifying pulmonary regurgitation using PW or CW Doppler (Lancellotti et al. 2010, 2013). Deceleration of the jet velocity is slow in mild and fast in severe pulmonary regurgitation, since in the latter situation there is fast equalization of pulmonary and right ventricular diastolic pressure (Feigenbaum et al. 2005; Lancellotti et al. 2013; Mertens et al. 2010; Yang et al. 2008). Therefore pressure half-time of the pulmonary regurgitation has been employed in adults to detect patients with severe insufficiency (Lancellotti et al. 2010, 2013; Yang et al. 2008). In patients with pulmonary regurgitation, pressure half-time < 100 ms predicts severe pulmonary regurgitation with good sensitivity and specificity (Silversides et al. 2003). The duration of pressure half-time is influenced however not only by the severity of pulmonary regurgitation but also by diastolic pulmonary artery pressure and right ventricular end diastolic pressure (Lancellotti et al. 2013).

Measurement of the peak diastolic gradient of pulmonary regurgitation according to the simplified Bernoulli equation has been shown empirically to correlate with mean pulmonary artery pressure (Mertens et al. 2010) *and provides important information in children with suspected pulmonary hypertension* (Fig. 7.15). For noninvasive estimation of mean pulmonary artery pressure, the central venous pressure or an estimate of right atrial pressure (e.g. 5 mmHg, as an equivalent of right ventricular end diastolic pressure) is added to the gradient of pulmonary regurgitation (Mertens et al. 2010). Clinically less important is the calculation of the pulmonary diastolic pressure, which can be derived from the measurement of end diastolic velocity of pulmonary regurgitation. Based on the simplified Bernoulli equation, it allows calculation of the end diastolic pressure difference between the pulmonary artery and the right ventricle. Addition of the end diastolic right ventricular pressure (which can be estimated with 5 mmHg–10 mmHg) to this gradient will give the diastolic pulmonary artery pressure (Feigenbaum et al. 2005; Mertens et al. 2010).

Doppler interrogation of the ductus arteriosus in infants with critical or significant pulmonary stenosis reveals exclusive LR-shunting. In the neonatal period, the gradient and flow velocities across the ductus will be low, due to the physiologically increased pulmonary vascular resistance.

Doppler interrogation of the interatrial communication in neonates with critical pulmonary stenosis is useful for delineation of timing and direction of shunting at atrial level. In the presence of critical pulmonary stenosis, significant RL-shunting may persist for days or even weeks following intervention or surgery and will result in some decrease of systemic oxygen saturation.

References

Aldousany AW, DiSessa TG et al (1989) Doppler estimation of pressure gradient in pulmonary stenosis: maximal instantaneous vs peak-to-peak, vs mean catheter gradient. Pediatr Cardiol 10(3):145–149

Alva C, Ho SY et al (1999) The nature of the obstructive muscular bundles in double-chambered right ventricle. J Thorac Cardiovasc Surg 117(6):1180–1189

Bashore TM (2007) Adult congenital heart disease: right ventricular outflow tract lesions. Circulation 115(14):1933–1947

Baumstark A, Fellows KE et al (1978) Combined double chambered right ventricle and discrete subaortic stenosis. Circulation 57(2): 299–303

Bove T, Francois K et al (2012) Assessment of a right-ventricular infundibulum-sparing approach in transatrial-transpulmonary repair of tetralogy of Fallot. Eur J Cardiothorac Surg 41(1): 126–133

Brown DW, McElhinney DB et al (2012) Reliability and accuracy of echocardiographic right heart evaluation in the U.S. Melody Valve Investigational Trial. J Am Soc Echocardiogr 25(4):383–392.e4

Buheitel G, Hofbeck M et al (1999) Incidence and treatment of reactive infundibular obstruction after balloon dilatation of critical pulmonary valve stenoses. Z Kardiol 88(5):347–352

Burch M, Sharland M et al (1993) Cardiologic abnormalities in Noonan syndrome: phenotypic diagnosis and echocardiographic assessment of 118 patients. J Am Coll Cardiol 22(4):1189–1192

Chaowalit N, Durongpisitkul K et al (2012) Echocardiography as a simple initial tool to assess right ventricular dimensions in patients with repaired tetralogy of fallot before undergoing pulmonary valve replacement: comparison with cardiovascular magnetic resonance imaging. Echocardiography 29(10):1239–1246

Chatelain P, Oberhansli I et al (1993) Physiological pulmonary branch stenosis in newborns: 2D-echocardiographic and Doppler characteristics and follow up. Eur J Pediatr 152(7):559–563

Collins RT 2nd (2013) Cardiovascular disease in Williams syndrome. Circulation 127(21):2125–2134

Duncan WJ, Fowler RS et al (1981) A comprehensive scoring system for evaluating Noonan syndrome. Am J Med Genet 10(1):37–50

Eicken A, Ewert P et al (2011) Percutaneous pulmonary valve implantation: two-centre experience with more than 100 patients. Eur Heart J 32(10):1260–1265

Elzenga NJ, von Suylen RJ et al (1990) Juxtaductal pulmonary artery coarctation. An underestimated cause of branch pulmonary artery stenosis in patients with pulmonary atresia or stenosis and a ventricular septal defect. J Thorac Cardiovasc Surg 100(3):416–424

Feigenbaum H, Armstrong WF et al (2005) Feigenbaum's echocardiography. Lippincott Williams & Wilkins, Baltimore/New York/London/Philadelphia

Freedom RM, Benson L (2004) Congenital pulmonary stenosis and isolated pulmonary insufficiency. In: Freedom RM, Yoo SJ, Mikailian H, Williams WG (eds) The natural and modified history of congenital heart disease. Elmsford, New York, Futura

Galal O, Al-Halees Z et al (2000) Double-chambered right ventricle in 73 patients: spectrum of the disease and surgical results of transatrial repair. Can J Cardiol 16(2):167–174

Gerlis LM (1999) The prevalence of bifoliate pulmonary valves. Cardiol Young 9(5):499–502

Grosse-Wortmann L, Yoo SJ (2010) Magnetic resonance imaging and computed tomography. In: Anderson RH, Baker EJ, Penny DJ et al (eds) Pediatric cardiology. Churchill Livingstone/Elsevier, Philadelphia

Koch A, Buheitel G et al (2003) Spectrum of arterial obstructions caused by one elastin gene point mutation. Eur J Pediatr 162(1): 53–54

Lancellotti P, Tribouilloy C et al (2010) European Association of Echocardiography recommendations for the assessment of valvular regurgitation. Part 1: aortic and pulmonary regurgitation (native valve disease). Eur J Echocardiogr 11(3):223–244

Lancellotti P, Tribouilloy C et al (2013) Recommendations for the echocardiographic assessment of native valvular regurgitation: an executive summary from the European Association of Cardiovascular Imaging. Eur Heart J Cardiovasc Imaging 14(7):611–644

Lee ST, Lin MH (2010) Color Doppler echocardiographic assessment of valvular regurgitation in normal infants. J Formos Med Assoc 109(1):56–61

Lemler MS, Ramaciotti C (2009) Anomalies of the right ventricular outflow tract and pulmonary valve. In: Lai WW, Mertens LL, Cohen MS, Geva T (eds) Echocardiography in pediatric and congenital heart disease. Blackwell Publishing Ltd, Chichester

Lindinger A, Schwedler G et al (2010) Prevalence of congenital heart defects in newborns in Germany: results of the first registration year of the PAN study (july 2006 to june 2007). Klin Padiatr 222(5):321–326

Luhmer I, Ziemer G (1993) Coarctation of the pulmonary artery in neonates. Prevalence, diagnosis, and surgical treatment. J Thorac Cardiovasc Surg 106(5):889–894

Martinez RM, Anderson RH (2005) Echocardiographic features of the morphologically right ventriculo-arterial junction. Cardiol Young 15(Suppl 1):17–26

McAleer E, Kort S et al (2001) Unusual echocardiographic views of bicuspid and tricuspid pulmonic valves. J Am Soc Echocardiogr 14(10):1036–1038

Mertens LL, Rigby ML et al (2010) Cross sectional echocardiographic and Doppler imaging. In: Anderson RH, Baker EJ, Penny DJ et al (eds) Pediatric cardiology. Churchill Livingstone/Elsevier, Philadelphia

Metcalfe K, Rucka AK et al (2000) Elastin: mutational spectrum in supravalvular aortic stenosis. Eur J Hum Genet 8(12):955–963

Momma K, Takao A et al (1986) Juxtaductal left pulmonary artery obstruction in pulmonary atresia. Br Heart J 55(1):39–44

Musewe NN, Robertson MA et al (1987) The dysplastic pulmonary valve: echocardiographic features and results of balloon dilatation. Br Heart J 57(4):364–370

Pankau R, Siebert R et al (2001) Familial Williams-Beuren syndrome showing varying clinical expression. Am J Med Genet 98(4): 324–329

Puchalski MD, Askovich B et al (2008) Pulmonary regurgitation: determining severity by echocardiography and magnetic resonance imaging. Congenit Heart Dis 3(3):168–175

Restivo A, Cameron AH et al (1984) Divided right ventricle: a review of its anatomical varieties. Pediatr Cardiol 5(3):197–204

Roberts AE, Allanson JE et al (2013) Noonan syndrome. Lancet 381(9863):333–342

Romano AA, Allanson JE et al (2010) Noonan syndrome: clinical features, diagnosis, and management guidelines. Pediatrics 126(4):746–759

Said SM, Burkhart HM et al (2012) Outcomes of surgical repair of double-chambered right ventricle. Ann Thorac Surg 93(1):197–200

Schwedler G, Lindinger A et al (2011) Frequency and spectrum of congenital heart defects among live births in Germany : a study of the competence network for congenital heart defects. Clin Res Cardiol Off J German Cardiac Soc 100(12):1111–1117

Silversides CK, Veldtman GR et al (2003) Pressure half-time predicts hemodynamically significant pulmonary regurgitation in adult patients with repaired tetralogy of fallot. J Am Soc Echocardiogr 16(10):1057–1062

Silvilairat S, Cabalka AK et al (2005a) Echocardiographic assessment of isolated pulmonary valve stenosis: which outpatient Doppler gradient has the most clinical validity? J Am Soc Echocardiogr 18(11):1137–1142

Silvilairat S, Cabalka AK et al (2005b) Outpatient echocardiographic assessment of complex pulmonary outflow stenosis: Doppler mean gradient is superior to the maximum instantaneous gradient. J Am Soc Echocardiogr 18(11):1143–1148

Snider RA, Serwer GA et al (1997) Echocardiography in pediatric heart disease. Mosby, St. Louis

So BH, Watanabe T et al (1996) Doppler assessment of physiological stenosis at the bifurcation of the main pulmonary artery: a cause of functional murmur in neonates. Biol Neonate 69(4):243–248

Turnpenny PD, Ellard S (2012) Alagille syndrome: pathogenesis, diagnosis and management. Eur J Hum Genet 20(3):251–257

Vogel M, Smallhorn JF et al (1988) An echocardiographic study of the association of ventricular septal defect and right ventricular muscle bundles with a fixed subaortic abnormality. Am J Cardiol 61(10):857–860

Wessel A, Pankau R et al (1994) Three decades of follow-up of aortic and pulmonary vascular lesions in the Williams-Beuren syndrome. Am J Med Genet 52(3):297–301

Yang H, Pu M et al (2008) Quantitative assessment of pulmonary insufficiency by Doppler echocardiography in patients with adult congenital heart disease. J Am Soc Echocardiogr 21(2):157–164

Zalzstein E, Moes CA et al (1991) Spectrum of cardiovascular anomalies in Williams-Beuren syndrome. Pediatr Cardiol 12(4):219–223